JACS
JOURNAL OF THE AMERICAN CHEMICAL SOCIETY

Article

pubs.acs.org/JACS

Racemization of a Chiral Nanoparticle Evidences the Flexibility of the Gold−Thiolate Interface

Stefan Knoppe, Igor Dolamic, and Thomas Bürgi*

Department of Physical Chemistry, University of Geneva, 30 Quai Ernest-Ansermet, 1211 Geneva 4, Switzerland

Supporting Information

ABSTRACT: Thiolate-protected gold nanoparticles and clusters combine size-dependent physical properties with the ability to introduce (bio)chemical functionality within their ligand shell. The engineering of the latter with molecular precision is an important prerequisite for future applications. A key question in this respect concerns the flexibility of the gold−sulfur interface. Here we report the first study on racemization of an intrinsically chiral gold nanocluster, $Au_{38}(SCH_2CH_2Ph)_{24}$, which goes along with a drastic rearrangement of its surface involving place exchange of several thiolates. This racemization takes place at modest temperatures (40−80 °C) without significant decomposition. The experimentally determined activation energy for the inversion reaction is ca. 28 kcal/mol, which is surprisingly low considering the large rearrangement. The activation parameters furthermore indicate that the process occurs without complete Au−S bond breaking.

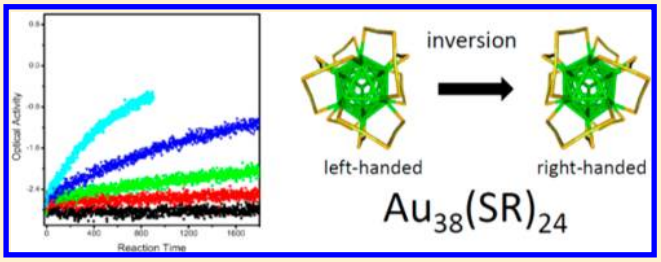

INTRODUCTION

Interest in thiolate-protected gold nanoparticles has grown tremendously in the past decade, triggered by potential applications in different branches of nanotechnology such as sensing, electronic devices, optics, catalysis, and biomedical applications. Nanometer-sized gold particles or clusters exhibit size-dependent catalytic, electronic, and optical properties[1−6] which are largely determined by their metal core. In addition, the protecting thiolate ligand shell can be functionalized in order to tune the (bio)chemical properties of the particles. It is evident that future applications of thiolate-protected gold nanoparticles will rely on the ability to engineer this ligand shell with molecular precision. Surprisingly, the structure of the gold−thiolate interface was determined only recently for thiolate-protected gold nanoclusters of defined constitution $Au_n(SR)_m$ (SR = thiolate) using X-ray crystallography.[7−10] The structures reveal the presence of a staple-type binding motif between gold and sulfur, in which a gold adatom is stabilized between two thiolate ligands.[11,12] The staples occur in two fashions, dimeric ($Au_2(SR)_3$) and monomeric ($Au(SR)_2$). Scanning tunneling microscopy work suggests that these staple motifs are also found on flat gold surfaces.[13,14] Trimeric staples ($Au_3(SR)_4$) have been proposed for ultrasmall clusters, in order to account for their extreme curvature.[15,16] It therefore emerges that the staples are a general and thermodynamically favored binding motif of thiolates on gold.

The ability to engineer the thiolate ligand shell of gold nanoparticles requires a deeper understanding of the properties of the staple motif that goes beyond its structure. Particularly, the flexibility of the gold−thiolate interface needs to be addressed. It is known that thiolates within the staples can be replaced (thiolate-for-thiolate exchange) when the particle is exposed to free thiols in solution.[17−24] Annealing is also a common technique in surface sciences to reorganize adsorbate molecules into self-assembled monolayers (SAMs).[25,26] Apart from that, important questions concerning the flexibility and stability of the staples within the ligand shell of gold nanoparticles remain unanswered, mainly due to the fact that it is difficult to address such questions experimentally. The exchange of the position of two thiolates on the surface of a gold particle, for example, is difficult to detect, because the initial and final states are identical and therefore cannot be distinguished by ordinary spectroscopic methods. An outstanding exception to this is chiroptical spectroscopy for processes that transform a chiral structure into its mirror image. Indeed, chirality has been found for thiolate-protected gold particles and clusters and was first reported in 1998.[27,28] Since then, quite a few studies have been carried out on the chiroptical properties of such systems,[17,19,29−35] but in those, chirality (or at least diastereomeric excesses[20]) was induced by chiral protecting ligands. Besides that, it turned out that the staple motifs can form a chiral pattern even if the thiol itself is achiral.[7,9,16,36]

Very recently, we succeeded in the first enantioseparation of the intrinsically chiral $Au_{38}(SCH_2CH_2Ph)_{24}$ and extended the method to the structurally unknown $Au_{40}(SR)_{24}$ cluster.[37,38] The Au_{38} cluster exhibits strong chiroptical responses with anisotropy factors $\Delta A/A$ of up to 4×10^{-3}, which is the largest ever observed for gold clusters. The Au_{38} cluster is of prolate shape covered by three monomeric and six dimeric staples. The latter are arranged in a chiral fashion to form two tri-blade fans

Received: June 9, 2012
Published: July 13, 2012

dx.doi.org/10.1021/ja3053865 | J. Am. Chem. Soc. 2012, 134, 13114−13120

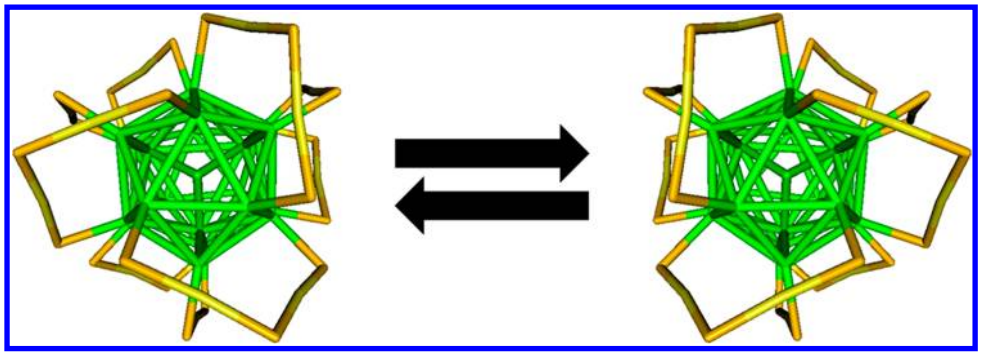

Figure 1. Schematic representation of the racemization reaction of $Au_{38}(SR)_{24}$ clusters along the principal axis of the cluster. In this scheme, the left-handed cluster (left) is converted into the right-handed enantiomer (right). The structures were created using the crystallographic data provided in ref 9. The $-CH_2CH_2Ph$ entities of the ligands were omitted for clarity. Color code: green, Au_{core}; yellow, Au_{adatom}; orange, S.

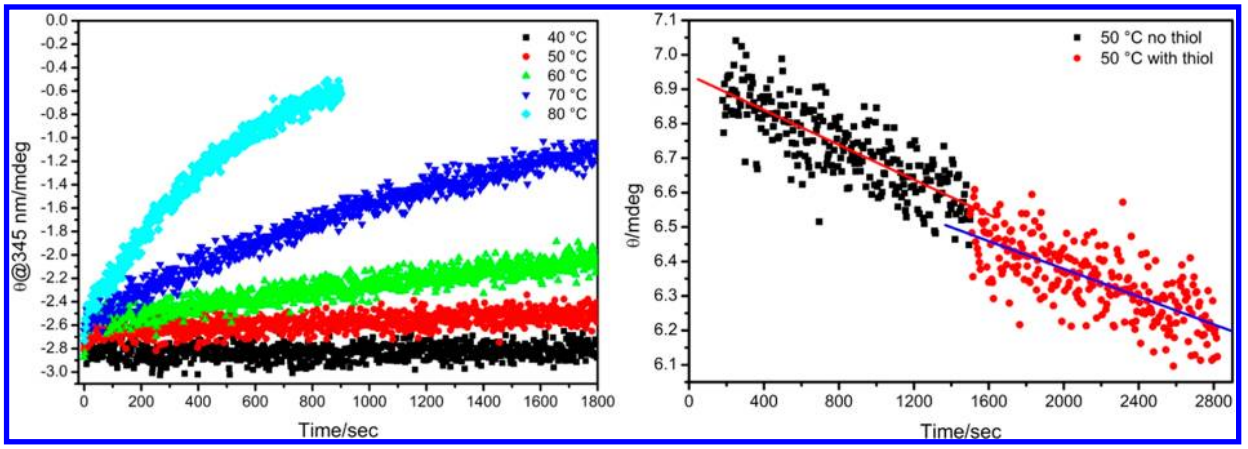

Figure 2. CD response at 345 nm of enantiopure $Au_{38}(SCH_2CH_2Ph)_{24}$. Left: Enantiomer 1 at different temperatures (initial concentration of enantiomer 1: 1.25×10^{-6} mol/L). The response is negative at 345 nm and approaches zero with time; the rate increases with temperature. Right: Enantiomer 2 at 50 °C. Black, heating of the pure enantiomer; red, addition of free 2-phenylethanethiol. The reaction is not accelerated; in contrast, it seems to be slowed, possibly due to a slight dilution effect upon thiol addition (see text).

at the poles of the cluster that rotate clockwise or counterclockwise (but both in the same sense, within one enantiomer), depending on the enantiomer. The ability to separate and store enantioseparated Au_{38} clusters at room temperature enables us to study their racemization using circular dichroism (CD) spectroscopy.[39] Racemization in $Au_{38}(SCH_2CH_2Ph)_{24}$ implies a considerable rearrangement of the ligand shell of the cluster, although the initial and final structures are identical except for their handedness (Figure 1). By following the temperature-dependent kinetics of the racemization, we were able to extract for the first time activation parameters for a well-defined rearrangement within the thiolate–gold interface of a thiolate-protected gold cluster.

METHODS

All chemicals were purchased from standard suppliers and used as received. Nanopure water (>18 MΩ) was used.

Synthesis and Isolation of *rac*-$Au_{38}(SCH_2CH_2Ph)_{24}$. *Step 1.*[19] Tetrachloroauric acid trihydrate (1 g) was dissolved in methanol (200 mL), and L-glutathione (3.1 g) was dissolved in water (100 mL). The solutions were combined at room temperature, resulting in a yellow-brown suspension that was then stirred at 0 °C for 15 min. A freshly prepared solution of sodium borohydride (1.1 g in 60 mL) was added all at once, and the reaction mixture was stirred at 0 °C for another 60 min. The resulting black clusters precipitated from the solution. The clusters were collected by centrifugation (5000 rpm, 10 min) and washed with methanol.

Step 2.[19] The clusters from step 1 were dissolved in 10 mL of water, and then acetone (10 mL) and 2-phenylethanethiol (15 mL) were added. The system was heated to 80 °C for 3 h. After the system cooled to room temperature, water and methylene chloride were added. The phases were separated, and the aqueous phase was discarded. The organic phase was washed with water another three times. The solvents were removed by rotary evaporation, and the clusters were precipitated from the excess thiol with methanol. The precipitate was washed with large amounts of methanol and filtered over a regenerated cellulose membrane (0.2 μm). The clusters were dissolved in methylene chloride, and the solvents were removed by rotary evaporation. The clusters were again washed with methanol. Overall, five washing cycles were performed. The clusters were then dissolved in methylene chloride and passed through a PTFE syringe filter (0.2 μm) to remove insoluble byproducts.

Step 3.[40] The purified products from step 2 were dissolved in a minimum amount of tetrahydrofuran and passed over a gel permeation column (GPC). The Au_{38} fraction was collected and refined several times until the UV–vis absorption properties were stable over the whole band and the MALDI mass spectrum showed only one signal. The clusters were washed with methanol (see step 2) and passed over a PTFE syringe filter prior to HPLC separation. The GPC column was packed as follows: a total of 45 g of BioRad BioBead S-X1 was suspended in 400 mL of tetrahydrofuran and allowed to swell for at least 3 h. The gel was put into a column (110 cm, 2.5 cm in diameter) equipped with a G4 glass frit and washed with THF until the eluting solvent was clear (about seven bed volumes). The bed height was about 90 cm. After each chromatographic run, the column was washed with ca. 1–2 bed volumes of tetrahydrofuran prior to reuse.

dx.doi.org/10.1021/ja3053865 | J. Am. Chem. Soc. 2012, 134, 13114–13120

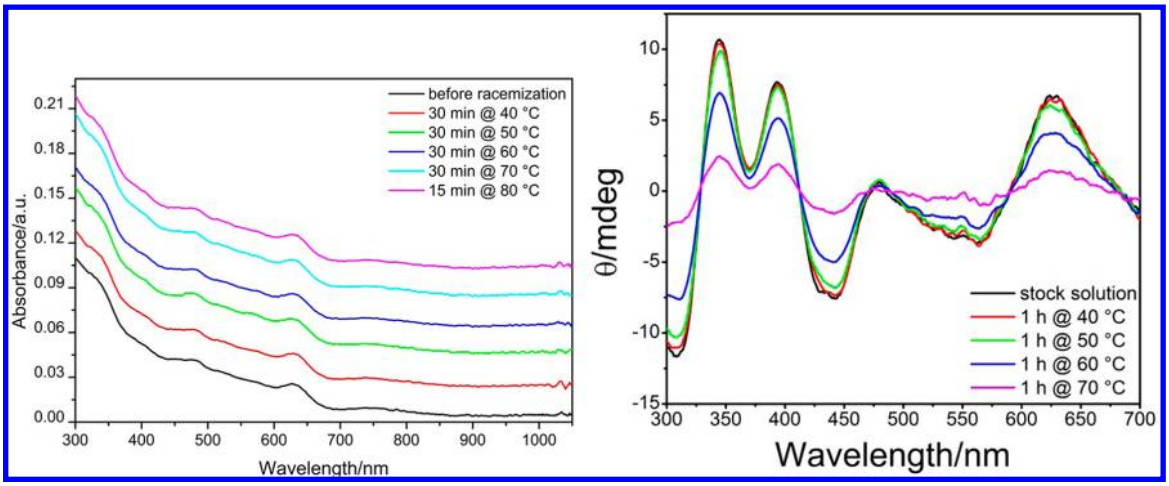

Figure 3. Left: UV−vis spectra (toluene) of enantiopure $Au_{38}(SCH_2CH_2Ph)_{24}$ before (black) and after racemization at elevated temperatures. The spectra show no hint of decomposition (30 min). The spectra are offset for clarity. Right: CD spectra of $Au_{38}(SCH_2CH_2Ph)_{24}$ (enantiomer 2) before (black) and after thermal treatment (1 h). The shape of the spectra is conserved, but the extent of chiroptical response is lowered with increasing temperature.

Characterization. UV−vis spectra were recorded on a Varian Cary 50 spectrometer. Quartz cuvettes of 10 or 5 mm path length were used (solvents: methylene chloride and toluene). CD spectra were recorded on a JASCO J-815 CD spectrometer. Full spectra were recorded in toluene or dichloromethane. For time-course measurements, the chiroptical response at 345 nm was followed in 2 s intervals at different temperatures (40, 50, 60, 70, and 80 °C, JASCO Peltier element, toluene, 5 mm path length), and the signal of blank toluene (55 °C) was subtracted.

HPLC. Chiral HPLC was performed on a JASCO 20XX HPLC system equipped with a Phenomenex Lux Cellulose-1 column (100 Å, 250 mm × 4.6 mm), and the eluting analytes were detected with a JASCO 2077plus UV detector (380 nm).[37] The analytes were dissolved in toluene and eluted with *n*-hexane:2-propanol (8:2) at a flow rate of 2 mL min^{-1}.

Racemization. A larger amount of enantiopure material was collected and dried by rotary evaporation. For this, the temperature was kept below 25 °C in order to avoid racemization prior to the experiment. A stock solution was made (concentration determined by comparing the absorption to those of solutions of known concentration) and split for racemization at different temperatures. Prior to heating, a CD spectrum was recorded for comparison. The samples were heated to 40, 50, 60, 70, and 80 °C for 30 min (15 in the 80 °C case), and the CD response at 345 nm was monitored in situ.

RESULTS AND DISCUSSION

Racemic $Au_{38}(SCH_2CH_2Ph)_{24}$ was prepared and isolated as described earlier, and UV−vis and MALDI data were in agreement with those reported (not shown).[19,37,40] Enantioseparation was performed using chiral HPLC, and the CD spectra of the isolated material were recorded.[37] A larger amount of material was collected and characterized. The UV−vis signature of the isolated enantiomers does not differ from that of the starting material, and the CD spectra of the separated enantiomers show a mirror image relationship.[37] We therefore conclude a nondestructive separation of the left- and right-handed enantiomers of $Au_{38}(SCH_2CH_2Ph)_{24}$.

For racemization studies, the enantiopure material was dissolved in a diluted stock solution (toluene). The concentration was determined by comparing the optical density spectrum of the solution to spectra of known concentration. Racemization was then performed, following the intensity of the CD signal at 345 nm over the course of 30 min (Figure 2, left). The measurements were performed at five different temperatures (40, 50, 60, 70, and 80 °C). In order to test the influence of free thiols, a sample was treated at 50 °C for 25 min, after which free 2-phenylethanethiol ($HSCH_2CH_2Ph$) was added, and the thermal treatment was continued for an additional 20 min (Figure 2, right). Again, the CD response was monitored at 345 nm; interestingly, no acceleration of the reaction was observed. In fact, a slight decrease in the reaction rate was observed, which may be attributed to a dilution effect (even though this should be minor, since 10 μL of thiol was added to about 2 mL of stock solution).

Temperature treatment has no significant influence on the UV−vis spectra of the clusters (Figure 3, left). This indicates stability of the clusters against decomposition at slightly elevated temperatures. The stability of the ordinary absorption spectra is in sharp contrast to the chiroptical responses (Figure 3, right). Treatment at elevated temperatures leads to significant decrease of the CD response. However, the shape of the CD spectrum is conserved. Calculation of anisotropy factors is in agreement with these observations (Figure S-1). We reason that the cluster survives temperature treatment without decomposition and undergoes racemization. This is supported by HPLC, which shows no significant peaks besides those of the enantiomers of the cluster (Figure S-2). The enantiopure cluster shows only one peak in the chromatogram. After thermal treatment, a second peak at the elution time of enantiomer **2** occurs. The peak grows in intensity with increasing temperature.

Since the concentration of the stock solution was identical for all racemization experiments, the time-dependent CD response at 345 nm is directly proportional to the enantiomeric excess (ee) of the solutions. Plots of ln(ee) versus time yielded straight lines (Figure S-3), thus indicating first-order kinetics (where ee is the enantiomeric excess of enantiomer **1** determined from the CD experiments). Rate constants $k(T)$ were gained by determining the initial reaction rates by linear fits. The Arrhenius plot (Figure 4) gives a linear fit (weighted linear regression), and the activation energy is determined to be 28.14 ± 0.53 kcal/mol. Derived thermodynamic activation parameters $\Delta H^{\ddagger}$, $\Delta S^{\ddagger}$, and $\Delta G^{\ddagger}$ are summarized in Table S-1. For 20 °C, $\Delta G^{\ddagger}$ = 25.55 ± 0.55 kcal/mol. The activation

dx.doi.org/10.1021/ja3053865 | J. Am. Chem. Soc. 2012, 134, 13114−13120

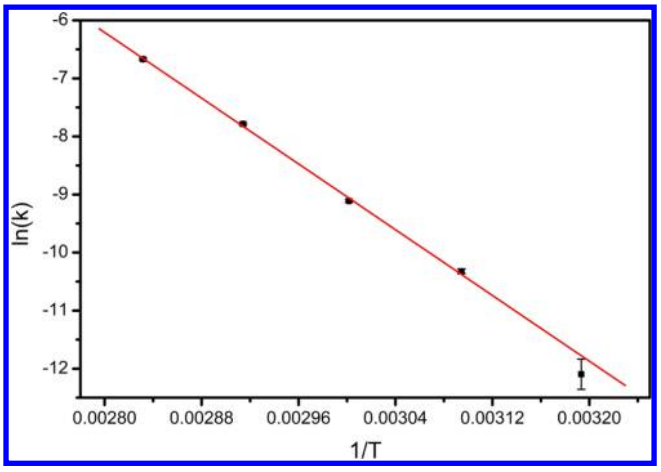

Figure 4. Arrhenius plot $\ln(k)$ vs $1/T$ for the racemization of enantiomer 1 of $Au_{38}(SCH_2CH_2Ph)_{24}$ at 40, 50, 60, 70, and 80 °C. The standard deviation for $\ln(k)$ is marked for each data point, and the data points were fit by a weighted linear regression. The extracted activation energy (slope) is E_a = 28.14 ± 0.53 kcal/mol.

entropy is very close to zero and positive (0.49 ± 0.08 cal mol^{-1} K^{-1}).

The findings of the UV–vis, CD, and HPLC experiments clearly show that the Au_{38} cluster undergoes a racemization reaction, which involves the inversion of the handedness of the fan-like structures formed by the dimeric staples at the poles of the cluster. This is the first observation of a reaction of this kind. The results furthermore show that, under the applied conditions, no significant decomposition takes place. Racemization is observed already at moderate temperatures. For example, at 80 °C it takes about 10 min to convert an enantiopure sample to one with about 50% ee. At 40 °C this is achieved within about one day.

The activation energy E_a and enthalpy of activation were determined to be slightly below 30 kcal/mol. This number is difficult to put in context due to the mere lack of data. A gold–sulfur bond affords ca. 50 kcal/mol.[41,42] State-of-the-art gradient-corrected density functional theory methods yield a binding energy of a thiolate radical to a gold atom, cluster, or the (111) surface of about 56 kcal/mol.[43−45] These values are significantly higher than the activation barrier we determined for the racemization of Au_{38}. On the other hand, Lavrich et al. determined the chemisorption enthalpy in the formation of SAMs of thiols and disulfides on Au(111) surfaces using thermal desorption measurements in a vacuum to be in the range of 30 kcal/mol.[46] This is close to the activation barrier we determined for racemization (but still higher by ca. 2 kcal/mol). The activation parameters are strictly associated with the reaction mechanism. Unfortunately, there is no direct information on the mechanism and the transition state available. However, a key question is whether the racemization involves complete Au–S bond breaking. Racemization could, for example, be achieved by breaking a bond between a surface atom and the protecting sulfur atom at the end of a dimeric staple, followed by replacing the bond between the core surface and the neighboring staple. This has to happen on both hemispheres of the cluster in order to achieve full inversion of

Scheme 1. Inversion of a Left-Handed Hemisphere through a Quasi-symmetric Intermediate to a Right-Handed Hemisphere, Following (Top) the S_N2-Type Mechanism[a] and (Bottom) the Proposed "Slide" Mechanism[b]

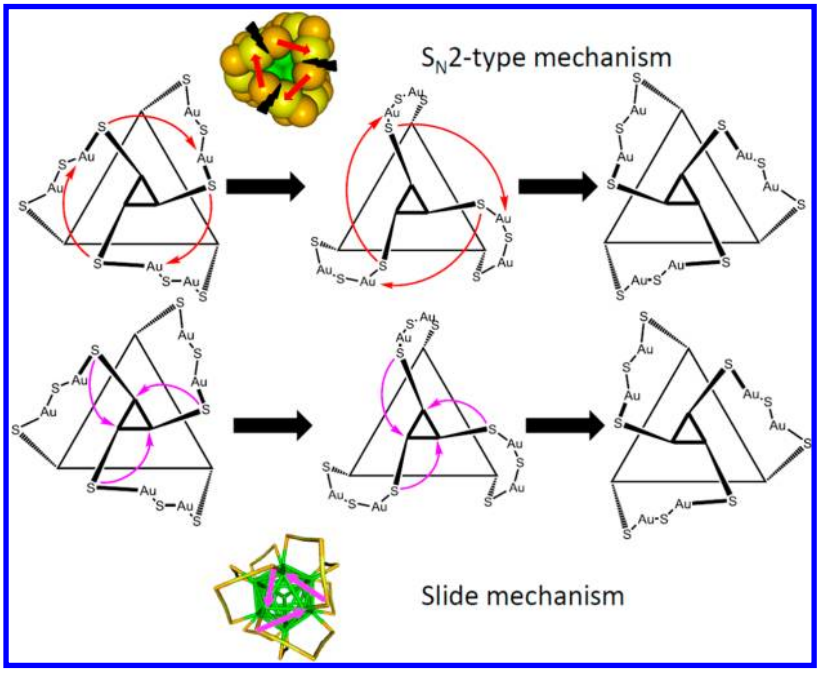

[a] Note that this scheme represents only one hemisphere; the other hemisphere is not necessarily affected by the inversion. Corners of the triangles are surface Au atoms; the second layer of binding monomeric staples is omitted. This can lead to the Pei intermediate (in which one hemisphere is right- and the other one left-handed). The space-filling structure at the top is the view along the principal axis of the cluster. Red arrows denote the sense of the attacking sulfur atoms toward Au adatoms in neighboring staples; black arrows highlight the bond that is broken during this process.

[b] Sliding of the sulfur atoms along the Au–Au (surface) bonds is highlighted by magenta arrows. The structure at the bottom is a wireframe representation of the cluster in top view, as it provides more insight into the movement of the atoms involved.

dx.doi.org/10.1021/ja3053865 | J. Am. Chem. Soc. 2012, 134, 13114–13120

Scheme 2. Idealized Potential Energy Surface of the Inversion of $Au_{38}(SR)_{24}$ Clusters, Following the Proposed Mechanisms[a]

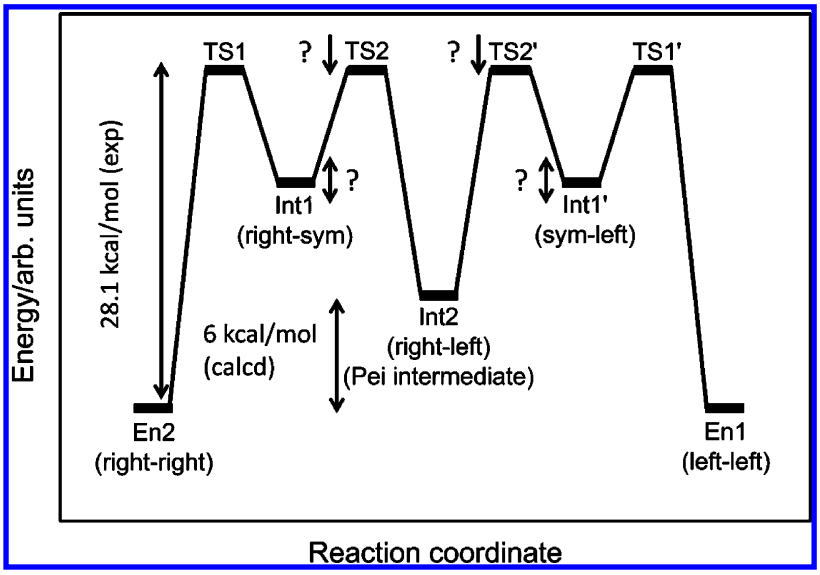

[a]The mechanism is based on the assumption that full inversion of the cluster is composed of two rather independent inversions of the individual hemispheres; Int2 = Pei intermediate (see text). The energy landscape is symmetric with respect to the chiral isomers. Note that the energies are arbitrary as exact values are unknown, except for the activation energy that we determined experimentally. The Pei intermediate was calculated to be destabilized by 6 kcal/mol.[36] The values of the other intermediates and transition states (TS2 and Int1) are unknown and may vary (indicated by question marks and arrows).

the structure. Several arguments indicate that a complete bond breaking is not involved in the racemization process. (i) The activation energy seems low for complete bond breaking, and even more so when considering that more than one Au−S bond needs to be broken and re-formed for the complete inversion of the handedness of the fan-like structures composed of dimeric staples. (ii) The addition of free thiol has no significant influence on the reaction rate. Free thiol could easily react with the free gold atom obtained after Au−S bond breaking. Also, free thiol may catalyze Au−S bond breaking. Both effects should influence the racemization rate, which is not observed. (iii) The activation entropy is very close to zero, which suggests a mechanism that is in accordance with a least-motion principle. The activation entropy is a measure of the available configurations of the transition state with respect to the initial state. The negligible activation entropy is therefore an argument against a fully broken bond in the transition state, since the associated entropy should differ considerably from that of the stable enantiomer. Instead of complete bond breaking, we suggest a mechanism that involves a series of intramolecular S_N2-type processes (see below). In this way, breaking and formation of bonds happen simultaneously.

The potential energy surface (PES) of a racemization reaction is symmetric with respect to the two enantiomers, neglecting very small effects due to parity violation.[47] In a recent article by Lopez-Acevedo et al.,[36] the structure of $Au_{38}(SR)_{24}$ was predicted to be chiral. (a similar structure was proposed by Pei et al.[48] even earlier, see below.) The key features of the structure with propeller-like arrangement of the dimeric staples at the poles are confirmed experimentally.[9] Note that in this structure the two propellers within one enantiomer of the cluster are of the same handedness. The structure proposed by Pei et al. shows opposite handedness of the dimeric (long) staple propellers, leading to a nonchiral structure. This structure is likely to be a stable intermediate in the racemization process and is reached through the inversion of the handedness of only one of the two propellers. In other words, this intermediate is reached if the two inversions of the propellers take place consecutively and not simultaneously. Since the two propellers are separated by three monomeric (short) staples, a consecutive mechanism seems plausible, according to

$$Au_{38}(\text{left}-\text{left}) \Leftrightarrow Au_{38}(\text{right}-\text{left}) \Leftrightarrow Au_{38}(\text{right}-\text{right})$$

where *right* and *left* denote the handedness of the propellers in the two hemispheres.

Lopez-Acevedo et al. calculated the energy of Au_{38}(right−left) (the "Pei intermediate") to be 0.26 eV (6 kcal/mol) higher than the energy of the chiral isomers. At room temperature, the equilibrium concentration of this intermediate structure is therefore too small for it to be observed, and in the kinetic experiments discussed here its concentration is always too small since it reacts fast toward the chiral structures.

The transition state (or an intermediate of higher energy) could be imagined as "symmetrized" on one hemisphere of the cluster, leaving the other one unattached (Scheme 1). With "symmetrized" we mean that the long staples, when viewed along the long axis of the cluster, do not turn left or right but are "straight" (see Scheme 1). This intermediate (we call this Au_{38}(right/left-sym), where "right/left" indicates helicity in one hemisphere and "sym" a straight arrangement in the other) can either react to form the Pei structure as intermediate of the whole racemization process or rearrange into the starting enantiomer. From the Pei intermediate, the PES must be symmetric with respect to the enantiomeric isomers. An idealized overview of the energetics of the full inversion is given in Scheme 2.

How are the intermediates formed? We can imagine two mechanisms that both proceed in two elementary steps according to the above-mentioned formation of the Pei intermediate. The first one involves two consecutive S_N2-type reactions in which a sulfur atom (binding to the cluster core)

dx.doi.org/10.1021/ja3053865 | J. Am. Chem. Soc. 2012, 134, 13114−13120

attacks a gold adatom in a neighboring staple. The second mechanism ("slide" mechanism) involves sliding of sulfur atoms on the gold cluster core surface (see below).

We first focus on the S_N2-type mechanism (marked with red arrows in Scheme 1). Since we assume a concerted associative mechanism rather than a dissociative one, bond breaking between sulfur and surface Au atoms should not occur. One may imagine the following: The free electron pair of the sulfur atoms directly binding to the cluster core attacks the closest Au adatom in a neighboring staple. As can be seen from the space-filling model in Scheme 1, the corresponding sulfur and gold adatoms are quite close. It is reasonable to assume this process happening at the poles of the cluster rather than close to the equator. This S_N2-type process might happen simultaneously for all three staples in one hemisphere (the other hemisphere may remain unattached). As a result, a straight arrangement of the long staples is achieved, which is not favored. From the straight arrangement, the staples would proceed to react a second time in a similar manner (again attacking the Au adatom in a neighboring staple, as highlighted in the second step in Scheme 1), leading again to a propeller-type arrangement. It may be noteworthy that the inversion of the first hemisphere may involve two elementary steps; the overall racemization of the cluster would involve four steps (compare the idealized PES in Scheme 2). As the sense of substitution in the second step is arbitrary, this second step leads to either the starting enantiomer or the Pei intermediate. In the latter case, the two propellers on the two hemispheres are of opposite handedness (as proposed by Pei et al.). This intermediate can further react by inverting either one of the two propellers and proceed to form either the starting enantiomer or the opposite one. Thus, the intermediate is symmetric with respect to the reaction. Note that in this mechanism the long staples mix with each other, meaning that thiolates that form one staple before the rearrangement find themselves in different staples afterward.

One may also imagine a mechanism where the staples stay intact and do not mix. In the "slide" mechanism (marked with magenta arrows in Scheme 1), the rearrangement proceeds via a concerted sliding of the sulfur anchoring points of the staples along the gold cluster surface (Scheme 1, bottom). Similar to the above-described S_N2-type mechanism, the "slide" mechanism is a two-step process. Starting from the left-handed propeller (Figure 1, left enantiomer), the handedness can be inverted by simultaneously sliding the three sulfur atoms at the pole of the cluster counter-clockwise along the corresponding Au–Au (surface) bonds (Scheme 1). This leads to the same intermediate as proposed above for the S_N2 mechanism. An analogous second counter-clockwise motion leads to the inversion. Note that one clockwise motion of the left-handed propeller would lead to the same anchoring points of the staples as two counter-clockwise moves, but in that case the staples would be tied up, and unwinding would imply breaking and re-forming bonds within the staples. Of course, mechanisms other than the two discussed above might be thought of based on elementary sliding and S_N2-type steps. One of these is further discussed in the Supporting Information (Scheme S-1).

Both the S_N2-type and "slide" mechanisms are striking for several reasons. (i) The intermediate is symmetric, and both enantiomers can be formed at the same rate. (ii) The reaction is strictly intramolecular, and the addition of thiols does not affect the mechanism. (iii) No decomposition of the clusters is observed under the applied conditions and time scales (longer heating may induce decomposition). (iv) The activation entropy is very close to zero, which suggests a mechanism that is in accordance with a least-motion principle. A dissociative mechanism would afford bond breaking and reformation, which goes along with huge motion. However, we have to stress that we do not have direct information about the mechanism, so the mechanisms described above remain proposals. Further studies—experimental and/or computational—on this are necessary. The described mechanisms both reflect the fact that the staples on a gold cluster surface are highly flexible and inversion can be achieved under mild conditions.

The synthesis of Au_{38} clusters used in this study involves a thermal etching process. Starting from L-glutathionate-protected precursors, the clusters undergo phase transfer upon complete ligand exchange. These are etched in excess thiol to form Au_{38} clusters (along with others). The etching is performed at 80 °C. As the activation energy is relatively low and racemization can be achieved at moderate heating within short time, this may explain why a racemate is found after the etching, even though a homochiral compound (L-glutathione) is present in the reaction mixture and could potentially act as a chiral inducer.

In conclusion, we performed racemization of enantiopure $Au_{38}(SCH_2CH_2Ph)_{24}$ clusters at different temperatures and determined the activation barrier (28.1 kcal/mol). Circular dichroism spectroscopy was used as a probe for racemization. The reaction is not accelerated by addition of free thiol, which indicates an intramolecular, concerted rearrangement process. The activation barrier for the racemization is relatively low, which reflects the flexibility of the ligand shell on a thiolate-protected gold cluster and leads to rearrangements at moderate temperatures. We propose two concerted, two-step mechanisms without complete Au–S bond breaking that both lead to a symmetric intermediate, which has been calculated before as a stable structure of $Au_{38}(SR)_{24}$.[48] The intermediate shows two tri-blade fans of dimeric staples of opposite handedness. The flexibility of the Au–S interface, as evidenced here by the racemization of a chiral cluster, has important implications for future applications of thiolate-protected gold clusters, e.g., for drug delivery and *in vivo* sensing (human body temperature ~36 °C) or as asymmetric catalysts.

■ ASSOCIATED CONTENT

Supporting Information

Additional HPLC and CD data, along with other content as described in the text. This material is available free of charge via the Internet at http://pubs.acs.org.

■ AUTHOR INFORMATION

Corresponding Author

Thomas.Buergi@unige.ch

Notes

The authors declare no competing financial interest.

■ ACKNOWLEDGMENTS

We thank Prof. Amala Dass (University of Mississippi) for additional MALDI mass spectrometry measurements. Prof. Stefan Matile (Geneva) is acknowledged for providing the CD spectrometer. We are grateful to The Swiss National Foundation and the University of Geneva for financial support.

REFERENCES

(1) Wyrwas, R. B.; Alvarez, M. M.; Khoury, J. T.; Price, R. C.; Schaaff, T. G.; Whetten, R. L. *Eur. Phys. J. D* **2007**, *43*, 91.
(2) Zhu, M.; Aikens, C. M.; Hollander, F. J.; Schatz, G. C.; Jin, R. *J. Am. Chem. Soc.* **2008**, *130*, 5883.
(3) Devadas, M. S.; Bairu, S.; Qian, H.; Sinn, E.; Jin, R.; Ramakrishna, G. *J. Phys. Chem. Lett.* **2011**, *2*, 2752.
(4) Devadas, M. S.; Kim, J.; Sinn, E.; Lee, D.; Goodson, T., III; Ramakrishna, G. *J. Phys. Chem. C* **2010**, *114*, 22417.
(5) Wu, Z.; Jin, R. *Nano Lett.* **2010**, *10*, 2568.
(6) Hakkinen, H. *Nature Chem.* **2012**, *4*, 443.
(7) Jadzinsky, P. D.; Calero, G.; Ackerson, C. J.; Bushnell, D. A.; Kornberg, R. D. *Science* **2007**, *318*, 430.
(8) Heaven, M. W.; Dass, A.; White, P. S.; Holt, K. M.; Murray, R. W. *J. Am. Chem. Soc.* **2008**, *130*, 3754.
(9) Qian, H.; Eckenhoff, W. T.; Zhu, Y.; Pintauer, T.; Jin, R. *J. Am. Chem. Soc.* **2010**, *132*, 8280.
(10) Zhu, M.; Eckenhoff, W. T.; Pintauer, T.; Jin, R. *J. Phys. Chem. C* **2008**, *112*, 14221.
(11) Whetten, R. L.; Price, R. C. *Science* **2007**, *318*, 407.
(12) Hakkinen, H.; Walter, M.; Gronbeck, H. *J. Phys. Chem. B* **2006**, *110*, 9927.
(13) Maksymovych, P.; Yates, J. T., Jr. *J. Am. Chem. Soc.* **2008**, *130*, 7518.
(14) Voznyy, O.; Dubowski, J. J.; Yates, J. T.; Maksymovych, P. *J. Am. Chem. Soc.* **2009**, *131*, 12989.
(15) Pei, Y.; Gao, Y.; Shao, N.; Zeng, X. C. *J. Am. Chem. Soc.* **2009**, *131*, 13619.
(16) Tlahuice, A.; Garzon, I. L. *Phys. Chem. Chem. Phys.* **2012**, *14*, 3737.
(17) Gautier, C.; Bürgi, T. *J. Am. Chem. Soc.* **2008**, *130*, 7078.
(18) Si, S.; Gautier, C.; Boudon, J.; Taras, R.; Gladiali, S.; Bürgi, T. *J. Phys. Chem. C* **2009**, *113*, 12966.
(19) Knoppe, S.; Dharmaratne, A. C.; Schreiner, E.; Dass, A.; Burgi, T. *J. Am. Chem. Soc.* **2010**, *132*, 16783.
(20) Knoppe, S.; Dass, A.; Burgi, T. *Nanoscale* **2012**, *4*, 4211 −4216.
(21) Dass, A.; Holt, K.; Parker, J. F.; Feldberg, S. W.; Murray, R. W. *J. Phys. Chem. C* **2008**, *112*, 20276.
(22) Jupally, V. R.; Kota, R.; Van Dornshuld, E.; Mattern, D. L.; Tschumper, G. S.; Jiang, D. E.; Dass, A. *J. Am. Chem. Soc.* **2011**, *133*, 20258.
(23) Fields-Zinna, C. A.; Parker, J. F.; Murray, R. W. *J. Am. Chem. Soc.* **2010**, *132*, 17193.
(24) Guo, R.; Song, Y.; Wang, G.; Murray, R. W. *J. Am. Chem. Soc.* **2005**, *127*, 2752.
(25) Schönherr, H.; Ringsdorf, H.; Jaschke, M.; Butt, H. J.; Bamberg, E.; Allinson, H.; Evans, S. D. *Langmuir* **1996**, *12*, 3898.
(26) Delamarche, E.; Michel, B.; Kang, H.; Gerber, C. *Langmuir* **1994**, *10*, 4103.
(27) Schaaff, T. G.; Knight, G.; Shafigullin, M. N.; Borkman, R. F.; Whetten, R. L. *J. Phys. Chem. B* **1998**, *102*, 10643.
(28) Schaaff, T. G.; Whetten, R. L. *J. Phys. Chem. B* **2000**, *104*, 2630.
(29) Gautier, C.; Burgi, T. *J. Am. Chem. Soc.* **2006**, *128*, 11079.
(30) Gautier, C.; Taras, R.; Gladiali, S.; Burgi, T. *Chirality* **2008**, *20*, 486.
(31) Gautier, C.; Burgi, T. *ChemPhysChem* **2009**, *10*, 483.
(32) Knoppe, S.; Kothalawala, N.; Jupally, V. R.; Dass, A.; Bürgi, T. *Chem. Commun.* **2012**, *48*, 4630.
(33) Zhu, M.; Qian, H.; Meng, X.; Jin, S.; Wu, Z.; Jin, R. *Nano Lett.* **2011**, *11*, 3963.
(34) Yao, H.; Miki, K.; Nishida, N.; Sasaki, A.; Kimura, K. *J. Am. Chem. Soc.* **2005**, *127*, 15536.
(35) Yao, H.; Fukui, T.; Kimura, K. *J. Phys. Chem. C* **2007**, *111*, 14968.
(36) Lopez-Acevedo, O.; Tsunoyama, H.; Tsukuda, T.; Hakkinen, H.; Aikens, C. M. *J. Am. Chem. Soc.* **2010**, *132*, 8210.
(37) Dolamic, I.; Knoppe, S.; Dass, A.; Bürgi, T. *Nature Commun.* **2012**, *3*, 798.
(38) Knoppe, S.; Dolamic, I.; Dass, A.; Burgi, T. *Angew. Chem., Int. Ed.* **2012**, *51*, 7589.
(39) Vachon, J.; Bernardinelli, G.; Lacour, J. *Chemistry* **2010**, *16*, 2797.
(40) Knoppe, S.; Boudon, J.; Dolamic, I.; Dass, A.; Burgi, T. *Anal. Chem.* **2011**, *83*, 5056.
(41) Nuzzo, R. G.; Zegarski, B. R.; Dubois, L. H. *J. Am. Chem. Soc.* **1987**, *109*, 733.
(42) Love, J. C.; Estroff, L. A.; Kriebel, J. K.; Nuzzo, R. G.; Whitesides, G. M. *Chem. Rev.* **2005**, *105*, 1103.
(43) Grönbeck, H.; Curioni, A.; Andreoni, W. *J. Am. Chem. Soc.* **2000**, *122*, 3839.
(44) Andreoni, W.; Curioni, A.; Grönbeck, H. *Int. J. Quantum Chem.* **2000**, *80*, 598.
(45) Krüger, D.; Fuchs, H.; Rousseau, R.; Marx, D.; Parrinello, M. *J. Chem. Phys.* **2001**, *115*, 4776.
(46) Lavrich, D. J.; Wetterer, S. M.; Bernasek, S. L.; Scoles, G. *J. Phys. Chem. B* **1998**, *102*, 3456.
(47) Quack, M.; Stohner, J.; Willeke, M. *Annu. Rev. Phys. Chem.* **2008**, *59*, 741.
(48) Pei, Y.; Gao, Y.; Zeng, X. C. *J. Am. Chem. Soc.* **2008**, *130*, 7830.